"Performance Analysis of Spatial Channel Model in fast fading"

Thesis submitted in partial fulfillment of the requirement for the award of

degree of

MASTER OF ENGINEERING

In

ELECTRONICS & COMMUNICATION ENGINEERING

Submitted by

SANDEEP SRIVASTAVA

Roll no. 800861027

Under the Guidance of

Ms. Surbhi Sharma

Assistant Professor

ECED

Thapar University

Electronics and Communication Engineering Department

Thapar University, Patiala-147004 (INDIA)

June 2010

CERTIFICATE

I, Sandeep Srivastava, hereby certify that the work which is being presented in this thesis entitled "**Performance Analysis of Spatial Channel Model in fast fading**" by me in partial fulfillment of the requirements for the award of degree of master of Engineering in Electronics & Communication from Thapar University (Deemed University), Patiala, is an authentic record of my own work carried out under the supervision of Ms. Surabhi Sharma.

The matter presented in this thesis has not been submitted in any other University/ Institute for the award of Master of Engineering.

(Sandeep Srivastava)
Signature of the Student
Date...5.7.10.....

This is certified that the above statement made by the candidate is correct to the best of my knowledge.

Surbhi Sharma
Assistant Professor,
ECED
Date...5.7.10.....

Dr. A.K. Chartterjee
Professor & H.O.D., ECED
Thapar University, Patiala
Date...12.7.10.....

Dr. R.K. Sharma
Dean of Academic Affairs
Thapar University, Patiala
Date...13/7/10

Acknowledgement

Any fruitful effort in a new work needs a direction and guiding hands that shows the way. I take this opportunity to express my sincere gratitude to Ms. Surbhi Sharma (Assistant Professor, ECED), Thapar University, Patiala for her suggesting new ways for implementing my ideas by his expert guidance throughout my work.

I express my sincere gratitude to Dr. Rajesh Khanna (Associate. Professor, ECED) Department of Electronics and Communication Engineering, for his suggesting new ways for implementing my ideas by his expert guidance throughout my work

I am further indebted to Dr. A. K. Chatarjee, Professor and Head, Department of Electronics and Communication Engineering, for his moral support at every step. I am also thankful to all the staff members of the Electronics & Communication Engineering Department for their full cooperation and help.

Finally, my thanks to everyone who has in some way or other helped me in completing this project successfully. I should not fail to mention my parents who have always been a source of inspiration. I am grateful to my friends for their valuable support and help.

Abstract

Future wireless communication systems will utilize the spatial properties of the wireless channel to improve the spectral efficiency and thus increase capacity. This is realized by deploying multiple antennas at both the transmitter and receiver. Development and analysis of communication systems utilizing the spatial properties of the channel requires channel models that properly reflect these characteristics.

Due to the unpredictable nature of the wireless channel, a common approach is to model its effects statistically. A few large world-wide cooperations, like the third generation partnership project (3GPP) have developed channel models intended for reference and standardization use. These models are partly based on some bulk parameters that describe the characteristics of the channel over larger areas of several wavelengths. Such parameters include shadow fading, angle spread, and delay spread, etc.

In the spatial channel model (SCM) these large-scale parameters are, however, assumed independent between separate links, i.e., between channels modelling the propagation between one mobile and several base stations, or between one base station and several mobiles. Such assumptions may be valid for single-link, singe-cell systems, where each communication link is sufficiently separated in either time or frequency. In practice, dependencies between parameters describing separate wireless channels is expected. Future systems will allow a dense frequency reuse, and results from system evaluations based on models with independent links may be inaccurate. Examples of this may be in systems that exploit the spatial nature of the channel, like multi-user scheduling using a single carrier, or macro-diversity systems deploying several base stations. Therefore, it is important to analyze multi-node measurements in order to extract and characterize this channel dependence.

The aim of this thesis is to investigate MIMO system capacity using the Spatial Channel Model (SCM) and Channel Fast Fading, Channel Capacity, Spatial Autocorrelation, Power delay profile for different channel environments, proposed by standardization bodies (3GPP-3GPP2) for third generation systems.

In principle, the MIMO systems capacity can increase linearly with the number of antennas. In this thesis, system model for investigating the MIMO system is first summarized.

The capacity of MIMO systems in SCM propagation scenarios (suburban macro-cell and urban micro cell) is then evaluated and compared with i.i.d. model results. The simulation results show that capacity of the more realistic SCM channels does not increase linearly with the number of antennas. Analyses on channel capacity variation with time, variation in spatial auto- correlation with time and its power delay profile have done.

TABLE OF CONTENTS

List of Figures

List of Tables

List of Abbreviations

1-D	One-Dimensional
2-D	Two-Dimensional
1G	First Generation
2G	Second Generation
3G	Third Generations
3GPP	Third Generation Partnership Project
3GPP2	Third Generation Partnership Project Two
AHG	ad-hoc group
AoA	Angle of Arrival
AoD	Angle of Departure
AS	Angle Spread
AWGN	Additive White Gaussian Noise
BER	Bit Error Rate
BS	Base Station
CDF	Cumulative Distribution Function
CDMA	Code Division Multiple Access
CSI	Channel State Information
dB	Decibels
FDMA	Frequency Division Multiple Access
GSM	Global System for Mobile communications
i.i.d.	Independent and Identically Distributed
LOS	Line-Of-Sight
MIMO	Multiple Input Multiple Output

MISO	Multiple Input Single Output
MS	Mobile Station
NLOS	Non-Line-Of-Sight
pdf	Probability Density Function
R_X	Receiver
SCM	Spatial Channel Model
SIMO	Single Input Multiple Output
SISO	Single Input Single Output
SNR	Signal to Noise Ratio
TDMA	Time Division Multiple Access
T_X	Transmitter

CHAPTER 1

Introduction

The first chapter introduces the system model and brief description of the component used in it.

1.1. Introduction

Wireless communication systems have made large advances since the first generation (1G) systems. Frequency Division Multiple Access (FDMA) was the main techniques used at that level. Similarly, Time Division Multiple Access (TDMA) and Code Division Multiple Access (CDMA) technique are widely used in today's communication systems, which is the second generation (2G) systems [1]. CDMA is also used in the third generation (3G) systems. These three main multiple access schemes are used to allow users to simultaneously share radio spectrum, which is an finite and essential resource of all wireless communications technologies. Now a days, the wireless system designers are faced with several challenges: the limitation of the radio spectrum and the complexity of wireless propagation environment, moreover the increasing demand for better quality of service (QoS) and higher transmission date rate. Designers have divided frequency, time and code. What is the next dimension that can be exploited to overcome the above challenges? Space may be the answer. In the 3rd generation (3G) and beyond-3G (B3G) wireless communication systems, higher data rate transmissions and better quality of services are demanded. This motivates the investigation towards the full exploitation of time, frequency, and more recently, space domains. By deploying spatially separated multiple antenna elements at both ends of the transmission link, multiple-input multiple-output (MIMO) technologies can improve the link reliability and provide a significant increase of the link capacity. It was further shown in [2] that the MIMO channel capacity grows linearly with antenna pairs as long as the environment has sufficiently rich scatterers. To approach the promised theoretical MIMO channel capacity, practical signal processing schemes for MIMO systems have been proposed, for example, space time processing and space-frequency processing. Both the link capacity and signal processing performance are

greatly affected by fading correlation characteristics of the MIMO channels.

1.2 MIMO System Capacity

MIMO system capacity has been the subject of intense research in the past decade [4, 6–8]. Both Foschini [7, 8] and Telatar [6] have shown that for i.i.d. channels MIMO system capacity increases linearly with the number transmit antennas and receive antennas rather than logarithmically. This result can be intuited as: MIMO systems exploit the spatial diversity benefits of the channel by transmitting data over a matrix rather a vector channel [4]. A good overview of MIMO systems is presented in [4, 5].

The work in [7–12] has been done under the assumption that only the receiver has perfect channel information. Therefore the equal power allocation scheme [4, 7, 8] was used to calculated capacity. [6] and [13] presented the waterfilling power allocation scheme as the optimal solution when the channel is perfectly estimated at both transmitter and receiver. There are many techniques that can be used to achieve channel knowledge at the transmitter, such as feedback from the receiver or through the reciprocity principle in a duplex system. In this thesis, the channel knowledge is assumed to be available at transmitter.

1.3 Channel Modelling

Channel modelling is a fundamental research area in wireless communication due to the complexity of the signal propagation process. It plays a crucial role in the investigation of MIMO system capacity [2, 3].

The independent and identically distributed (i.i.d.) channel model has been used by researchers to derive the useful bounds of MIMO capacity [6–9,13]. As a stochastic channel model, the i.i.d. channel is the simplest and the most common channel model. Many different MIMO channel models have been presented in [14]. MIMO channel models can be classified in many different ways. The MIMO channel models can be divided into wideband and narrowband by considering the system band width [14]. In the wideband channel model, the channel is assumed to have different channel responses for different frequencies, so that the channel is a frequency selective fading channel. On the contrary, the narrowband channel model is assumed to have

an equal response over the system bandwidth. By considering the characteristics of the channel parameters, the MIMO channel models can be divided into non-physical and physical models [14]. The non-physical models use non-physical channel parameters based on the channel's statistical characteristics. However, the physical model uses some crucial physical parameters, such as Angle of Arrival (AoA), Angle of Departure (AoD) and Time of Arrival (ToA) to model the channel. The examples of physical narrowband channel models are 'One-Ring' and SCM channel models. As compared to i.i.d. channel model, the 'One-Ring' channel model takes into account the inter-element distance which makes it possible to study mutual coupling and correlation effects [10, 12]. The SCM (Spatial Channel Model) is an example of a more realistic channel model [19]. It is a standardized model developed by 3GPP-3GPP2 spatial channel model (SCM) ad-hoc group (AHG), which are standardization bodies for 3G cellular systems [18]. This model allows us to perform system level simulations, and offers three propagation scenarios for investigation: suburban macro-cell, urban macro-cell and urban micro-cell [18].

1.4 Aims of this Thesis

For different channel environments, proposed by standardization bodies (3GPP-3GPP2) for third generation system, the main objective of this thesis is

- To investigate MIMO system capacity using spatial channel model in Fast Fading
- To investigate channel capacity variation with time.
- To investigate variation in spatial autocorrelation with time.
- To generate its power delay profile

1.5 Thesis Organization

This *chapter* has provided an introduction of this thesis. It has explained the motivation and aims of this thesis. The remainder of this thesis is organized as follows.

In *chapter 2*, the work done in this field is shown. This is useful to understand the basics of this thesis.

In *Chapter 3*, the methodology of this thesis is presented. The system model for

MIMO systems is illustrated. The i.i.d., 'One-Ring and the SCM channel model are described in detail. The MIMO system capacity results are summarized for two different conditions: the channel information is not available at the transmitter and the channel information is available at the transmitter. The effects of mutual coupling and normalization methods are discussed. Some important performance measures are described at the end of the chapter.

In *Chapter 4*, the capacity results of the SCM channel model are presented. The effect of environments on channel is shown and the effects of number of antennas on MIMO capacity under the SCM channel are discussed. The effect of SNR on the capacity is also investigated. The capacities of suburban macro-cell and urban micro-cell are compared.

Finally, *Chapter 5* summarized the main thesis contribution and provide suggestions for future work.

Chapter 2

Literature Review

This chapter surveys some important studies in the field of our research outlines the main ideas contained in them.

David Gesbert et. al. [4] reviews the major features of MIMO links for use in future wireless networks. Information theory reveals the great capacity gains which can be realized from MIMO. Whether they achieve this fully or at least partially in practice depend on a sensible design of transmit and receive signal processing algorithms. As new and more specific channel models are being proposed it will useful to see how those can affect the performance tradeoffs between existing transmission algorithms and whether new algorithms, tailored to specific models, can be developed.

Wei Zhang [6] presents that if the channel transfer matrix is fixed and both known to the transmitter/ receiver, through some joint processing, we can achieve the capacity of this type of channel. In the fading environment, under the assumption of independent fades and noises at the different antennas, the capacity gain of multi-antenna systems over single-antenna systems can be very large. For example, if the number of receiving antenna equals the number of transmitting antenna, the capacity grows approximate linearly with this number when it is large, which does not occur in the fixed transfer matrix situation.

Shihai Shao et. al. [7] proposed a modified Vertical-Bell Labs Layered Space-Time (V-BLAST) system, where different delay offsets are intentionally applied to the spatially multiplexed data streams in order to improve bit error rate (BER) performance. The proposed system can use only one receive antenna to recover the transmitted information by zero forcing (ZF) detection, whereas the conventional synchronous V-BLAST system requires that $M_r \geq M_t$ (where M_t and M_r are the number of transmit and receive antennas, respectively). Compared with the conventional synchronous V-BLAST system, the modified system can achieve M_{rth} order diversity using ZF detection. Although delay

offsets in the system introduce an attenuation factor which decreases the instantaneous signal-to-noise ratio (SNR), the BER performance of the modified system with proper system parameters demonstrates a performance improvement over the conventional synchronous V-BLAST system.

G. J. Foschini et. al. [8] presented, that exploitation of multi element arrays can greatly advance indoor (and inter building) wireless data communications. Antenna lattices can pave the surface of transmitter and receiver spaces and two states of polarization are available. e.g., for indoor wireless LANs, we can anticipate bit rates far beyond where they are today where very little of the diversity that is possible is used. Where LAN systems may achieve 10's of Mbps in 20 MHz in the near term, in the long term, with the large n values that are possible. Gbps bit rates may be possible in such a bandwidth. It is also clear from our results that, by far, most of the great improvement in bit rate will come from processing spatially (compared to the incremental but nonetheless worthwhile advances in spectral efficiency employing existing antenna systems).

Herv´e Ndoumb`e Mbonjo et.al [9] investigate a MIMO channel that includes antenna coupling and derive the correlation matrix of the channel matrix in dependence on both antenna coupling and spatial correlation and shows mathematically that the impact of the coupling on the capacity can easily be studied with the aid of the eigenvalues of the coupling matrices. The MIMO channel capacity with antenna coupling is influenced by two effects if spatial correlation is not considered: 1) reduced element spacing yields loss in the rank of the channel matrix and hence a decrease of the capacity, 2) reduced element spacing can yield an increase in transmitted and/or received power and thus an increase of the capacity. Arrays should be designed in order to find a good tradeoff between these two effects. Under transmit power constraints and if also spatial correlation is taken into account, the capacity of the channel without coupling could not be exceeded for the investigated cases.

Da-shan Shiu et .al. [10] modeled the multipath propagation environment with an abstract model and derived the fading correlation as a function of the geometrical parameters of

the MEA (Multi-Element Antenna), including antenna spacing, antenna arrangement, angle spread, and the angle of arrival. They showed that the capacity of an (n, n) MEA is the sum of the capacities of n SISO subchannels whose power gains are the eigenvalues of HH^t , where H is the channel matrix. Their result shows that the stronger the fading correlation, the larger the statistical disparity is between the eigenvalues of HH^t. As a result, some subchannels have gains too small to convey information at any significant rate. They defined effective degrees of freedom to represent the number of subchannels that actively contribute to the overall MEA capacity. There results lead to insights as to how the geometry of the antenna set and the propagation environment affects the MEA capacity. They found that the angle spread and the BS antenna separation perpendicular to the direction of wave arrival dominate the channel correlation. The channel capacity and effective degrees of freedom (EDOF) decrease as the angle spread and for antenna spacing decrease. Thus they recommend broadside MEAs for directional coverage and hexagon MEAs for omnidirectional coverage.

Bjnrm Olav Hogstad et.al. [11] simulated the MIMO channel capacity for various propagation scenarios using the one ring scattering model. The space-time correlation properties between the time variant complex channel gains have been taken into account. Simulation results show an excellent correspondence between the statistical average and the time average of the capacity. Hence, the capacity seems to be mean ergodic. Another important observation is that the PDF of the capacity is independent of time. Simulation results show that increasing the distance between antenna elements at the BS and/or the MS can have a minor negative influence on the capacity.

Thomas Svantesson et. al. [12] studied the capacity of multiple element antenna systems, focusing on the effect of antenna spacing at the mobile terminal. In particular, the effect of mutual coupling between antenna elements were considered, and its effect on the correlation between channel coefficients and thereby on the capacity of such systems. Contrary to earlier claims regarding the effect of mutual coupling on capacity of MEA systems, they showed results to support the conclusion that coupling can in fact have a decorrelating effect on the channel coefficients and thereby also increasing the capacity.

David Gesbert et. al. [13] reviews the major features of MIMO links for use in future wireless networks. Information theory reveals the great capacity gains which can be realized from MIMO. It is clear that the success of MIMO algorithm integration into commercial standards such as 3G, WLAN, and beyond will rely on a fine compromise between rate maximization (BLAST type) and diversity (space time coding) solutions, also including the ability to adapt to the time changing nature of the wireless channel using some form of (at least partial) feedback. To this end more progress in modeling, not only the MIMO channel but its specific dynamics, will be required. As new and more specific channel models are being proposed it will useful to see how those can affect the performance tradeoffs between existing transmission algorithms and whether new algorithms, tailored to specific models, can be developed. Finally, upcoming trials and performance measurements in specific deployment conditions will be key to evaluate precisely the overall benefits of MIMO systems in real-world wireless scenarios such as UMTS.

Matthias P¨atzold et. al. [15] proposed an efficient and flexible deterministic simulation model for MIMO frequency nonselective Rayleigh mobile fading channels, where both the BS and the MS are equipped with an antenna array. The simulation model has been derived from a non realizable stochastic reference model by extending the concept of deterministic channel modelling with respect to MIMO fading channels. This MIMO channel simulator takes the Doppler effect and given spatial correlation properties into account. The proposed procedure for the design of deterministic MIMO channel simulators provides a fundamental framework for the test, optimization, design, and analysis of multi-element antenna systems. Moreover, the new MIMO channel simulator enables the simulation of sample functions of the channel capacity. From the simulation of the MIMO channel capacity, one can determine, for example, how often the capacity crosses a given threshold from up to down (or from down to up) within one second, or the expected value for the length of time intervals in which the channel capacity is below a given threshold.

Thomas Svantesson [16] presents a Multi-Input Multi-Output (MIMO) spatio temporal channel model for simulation of multi-element multi-polarized antenna systems. The model is based on EM scattering, thereby including many of the channel characteristics encountered in practice. By combining results from rough surface scattering and a dyad formulation of the scattering properties from a dielectric plate, a compact description of the polarization properties of the channel was obtained. Since the properties of the antenna are also included in the model, studies of MIMO systems employing dual-polarized antennas and other antenna arrangements are possible using the channel model. The model is also suited for analyzing channel prediction schemes and different feedback strategies for systems employing transmit diversity since the model naturally incorporates the time evolution of the channel.

B.K. Lau et. al. [19] investigated the impact of mutual coupling on capacity for compact MIMO systems. They found that for the case of wideband systems, the frequency dependence of the dipole antenna system can degrade the capacity performance at close antenna separation, as compared to the narrowband case. This is due to the frequency response of the matching network, which is not exactly matched to that of the antenna system over a finite bandwidth. Therefore, capacity performance in the presence of mutual coupling can differ between the narrowband and wideband cases.

J. Gong et. al. [20] derived the path gain and the covariance matrix under the assumptions that the total transmit power is constant and that each kind of receive antenna receives the same power when the same incident waves are uniformly distributed around the antenna. When the linear transmit array and the linear receive array lie to broadside each other, the microstrip array produces lower correlation than the dipole array.

Bruno Clerckx et. al. [22] analyzed the impact of mutual coupling on the channel capacity and the performance of spatial multiplexing (Maximum Likelihood detector and V-BLAST) and transmit diversity (Space-Time Block Coding). Antenna coupling induces two effects which seem to never appear simultaneously: the increase of element gain and channel decorrelation. Spatial multiplexing is shown to be more influenced by the decorrelation effect.

Salman Durrani et. al. [23] provided and compared results for the average SIR improvement for linear and circular arrays of half-wavelength spaced dipoles, which can be part of a base station of a CDMA cellular communication system. Two cases, one where mutual coupling is neglected and a second where mutual coupling is included, have been considered. They have shown that there is an improvement in SIR as N increases. In comparison, for a full angular range surrounding a base station, a circular array provides a more uniform improvement in terms of SIR than a linear array. Also the obtained results have shown that mutual coupling degrades the SIR improvement capability of the linear array, particularly in the broadside direction. In contrast, mutual coupling has little effect on the SIR improvement capability of the circular array for the assumed element spacing of half-wavelength.

P. N. Fletcher et. al. [24] presents that the couplings between elements results in distortion of the radiation patterns of the elements when embedded in an MEA. Pattern diversity was thought to further decorrelate spatial fading and give increased MlMO channel capacity. For the linear array considered, the pattern diversity is a result of coupling between elements and hence is a result of additional correlations between elements which actually reduces MIMO channel capacity.

Volker Jung nickel [26] present that wide-band radio channel measurements at 5.2 GHz with four transmit and four receive antennas at variable element spacing are reported, aiming to evaluate the potential of compact antenna arrays at mobile terminals and show that, for an element spacing $d < (0.5\text{-}\lambda)$ (down to $0.2\text{-}\lambda$), the link capacity is not smaller than that for much larger. This is explained by the observation that mutual coupling changes the radiation patterns of closely spaced antenna elements, individually. Compact multi antenna terminals may thus become practical.

Jon W. Wallace et. al. [30] presented a rigorous network-theory frame-work for the analysis of mutual coupling in MIMO wireless communications. A detailed network model was used to develop a new mutual information expression and radiated power constraint accounting for this antenna coupling. Closed-form derivation of the system capacity was made possible by relating the mutual information maximization problem to the multiport conjugate matching solution. This new method includes the effect of mutual

coupling, and the resulting capacity expression provides a true upper bound on system performance.

Jiangang Lv et. al. [31] present the MIMO system capacities using 2D ray tracing in NLOS indoor environment and indoor environment with LOS path were analyzed and also compared with the i.i.d. Rayleigh capacities. The results shows that different propagation environment affect the capacity greatly.

Richard B. Ertel et. al. [33] provided a review of a number of spatial propagation models. These models can be divided into three groups: 1. General statistically based models, 2. More site-specific models based on measurement data, 3. Entirely site-specific models. The first group of models (Lee's Model, Discrete Uniform Distribution Model, Geometrically Based Single Bounce Statistical Model, Gaussian Wide Sense Stationary Uncorrelated Scattering Model, Gaussian Angle of Arrival Model, Uniform Sectored Distributed Model, Modified Saleh Valenzuela's Model, Spatio Temporal Model) are useful for general system performance analysis. The models in the second group (Extended Tap Delay Line Model and Measurement Based Channel Model) can be expected to yield greater accuracy but require measurement data as an input. An example from the third group of models is Ray Tracing, which has the potential to be extremely accurate but requires a comprehensive description of the physical propagation environment as well as measurements to validate the models.

Thomas Svantesson [33] presents an analytical expression for the correlation between different modes and it was found that the correlation is low enough to yield a diversity gain. Furthermore, the channel capacity of a MIMO system employing multiple antennas or modes at the MS and BS was simulated using a spatial channel model. It was found that the multimode antenna offers capacity gains similar to that of the array antenna in several MIMO scattering environments.

Mansoor Shafi et. al. [35] present a novel approach to describe a MIMO cross polarized channel. This consists of defining a composite channel coefficient that is a scaled sum of

2D and 3D components. The 3D component is new and aims to model indoor and in vehicle situations.

Andreas F Molisch et. al. [37] demonstrated the importance of far scatterer clusters for the correct modeling of MIMO channels. They have demonstrated that far scatterer clusters frequently occur in urban environments, and that they cannot be replaced by an "equivalent" increase of the angular spread of the scatterer cluster around the MS.

Cheng-Xiang Wang et.al. [38] compare the spatial temporal correlation characteristics of the 3GPP SCM and KBSM at three levels. Theoretical studies clearly show that the spatial CCF of the SCM is related to the joint distribution of the AoA and AoD, while the KBSM calculates the spatial CCF from independent AoA and AoD distributions. Under the conditions that the number of sub paths tends to infinity in the SCM, two correlated links share one antenna at either end, and the same set of angle parameters is used, the two models tend to be equivalent.

R. Michael Buehrer et. al. [39] presents a spatial channel model for IMT-2000 systems as well as measurement results for 1.2MHz wide wireless channels using an eight element linear array at two different frequencies. The spatial channel model is a spatial extension of the commonly known IMT-2000 temporal (i.e., delay profile) model. The measurement results are used to characterize the spatial aspects of the wireless channel and are used to verify the model.

Daniel S. Baum [40] presents a report on the interim beyond-3G (B3G) channel model developed by and used within the European WINNER project. The model is a comprehensive spatial channel model for 2 and 5 GHz frequency bands and supports band widths up to 100 MHz in three different outdoor environments.

Hui Xiao et. al. [41] proposed a further extension to the 3GPP SCM to investigate the time variation of the wideband channels in an outdoor scenario. By considering more

parameters that influence the instantaneous channel matrix, and hence the channel correlation matrix, the NE-3GPP SCM can more realistically simulate the time variation of the wideband channels than the IB3G SCM.

Lusina, P. et. al. [42] propose that a significantly different performance can be expected under the same link parameters, depending on which channel model is assumed and also show that some models may be preferred because of the insight they offer or their advantage in terms of simplicity.

Min Zhang et. al. [43] presents a generalized methodology to derive the spatial correlation when the angles of arrival (AoA) and angles of departure (AoD) are either independent or partly correlated.

Chapter 3

Capacity Analysis of Antenna Systems

In 3rd chapter, channel model, channel capacity, and fading have been explained briefly.

3.1 Spatial Channel Model

The SCM (spatial channel model) is a spatial extension of the commonly known IMT-2000 (IMT-2000, "International Mobile Telecommunications",) temporal (i.e., delay profile) model. It is a so-called geometric or ray-based model based on stochastic modeling of scatterers. It defines three environments (Suburban Macro, Urban Macro, and Urban Micro) where Urban Micro is differentiated in line-of-sight (LOS) and non-LOS (NLOS) propagation. There is a fixed number of 6 "paths" in every scenario, each representing a Dirac function in delay domain, but made up of 20 spatially separated "sub-paths" according to the sum-of-sinusoids method. Path powers, path delays, and angular properties for both sides of the link are modeled as random variables defined through probability density functions (PDFs) and cross-correlations. All parameters, except for fast-fading, are drawn independently in time, in is termed as "drops". SCM is also the some modifications of the generation of the wideband fast fading channel matrix, such as the consideration of the time variant sub-path phases at the mobile station (MS), the consideration of the powers of the time variant multi-paths, and the generation of different last bounce distances for the mid-paths within each path. The Spatial Channel Model shows the spatial separability at the link and system levels, but not at the cluster level since its spatial correlation is related to the joint distribution of the angle of arrival (AoA) and angle of departure (AoD). The distortion caused by the wireless mobile channel can he described by three main parameters: (1) Doppler spread, (2) delay spread, and (3) angle spread. Doppler spread describes the dispersion of the transmitted signal experiences in the frequency domain, or equivalently the temporal fading. The delay spread describes the temporal spreading observed at the receiver or equivalently the frequency dependent fading. Finally, the angle spread describes the angular spreading observed at the receiver or equivalently the spatial dependent fading experienced.

Traditionally, wireless channel models have incorporated the first two parameters, but have ignored the third[39]. The SCM provides more insights of the variations of different MIMO channel realizations, but the implementation complexity is relatively high.

3.2 System Model

In a wireless system, a signal transmitted into the channel interacts with the environment in a very complex way. There are reflections from large objects, diffraction of the electromagnetic waves around objects, and signal scattering. The result of these complex interactions is the presence of many signal components, or multipath signals, at the receiver. Another property of wireless channels is the presence of Doppler shift, which is caused by the motion of the receiver, the transmitter, and/or any other objects in the channel.[33]

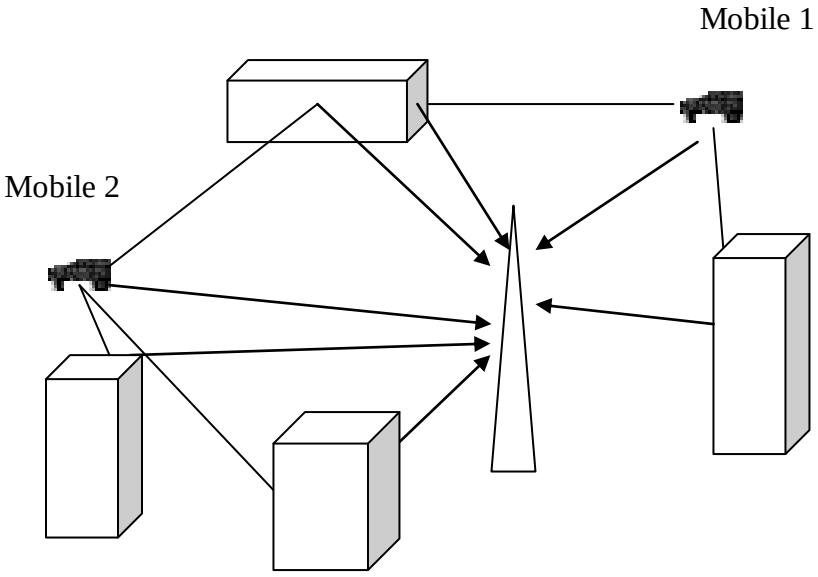

Figure 3.1 The multipath environment with two mobile stations.

A simplified pictorial of the multipath environment with two mobile stations is shown in Fig.3.1. Consider a narrow-band single user MIMO system with N_T transmit and N_R receive antennas. The antennas are assumed to be omnidirectional, which means that the antennas transmit and receive equally well in all directions. The linear link model between the transmit and receive antennas can be represented in the vector notation as

$$\mathbf{y} = \mathbf{Hx} + \mathbf{n} \tag{3.1}$$

where $\mathbf{y}$ is the $N_R \times 1$ received signal vector, $\mathbf{x}$ is the $N_T \times 1$ transmitted signal vector, n is the $N_R \times 1$ complex Gaussian noise vector with zero mean and equal variance, which is equal to σ^2, and $\mathbf{H}$ is the $N_R \times N_T$ normalized channel matrix, which can be represented as

$$\boldsymbol{H} = \begin{pmatrix} h_{11} & \cdots & h_{1Nt} \\ \vdots & \ddots & \vdots \\ h_{Nr1} & \cdots & h_{Nrt1} \end{pmatrix} \tag{3.2}$$

Each element h_{mn} represents the complex gains between the n^{th} transmit and m^{th} receive antennas.

3.3 Main Parameter affecting channel model

The measurement of system performance is often based on the statistical properties of the channel, and ideal antennas are assumed at both the transmitter and the receiver. A key requirement necessary to attain MIMO capacity is to have the signals associated with each link end uncorrelated. The correlation among antennas will be reduced if there are a large number of scatterers in the environment, which cause multiple copies of the signal to add randomly at the receiver. Increasing the separation between the antenna elements will also reduce correlation by ensuring that the multipath components arriving at, or departing from, each antenna element are sufficiently different. Realistic modelling of these two effects lies at the core of accurate prediction of MIMO systems. For MIMO systems, the electromagnetic coupling among the antenna elements may have significant affect the correlation of the signals at the output of each antenna, especially in small hand-held devices. Channel parameters are explained below which affect the channel model.

3.3.1 Link geometry and statistics

An illustration of a 2 × 2 MIMO link is shown in Fig. 3.2. It consists of a uniform linear array (ULA) with two elements each at the transmitter (T_x) and receiver (R_x). Only the azimuth plane is described both in our array geometry and in our channel models. The

t_x and r_x correspond to the T_x and R_x, respectively. The geometric parameters of our model are as follows. The antenna element separation is denoted by d and is measured in distances of wavelengths (λ) based on the

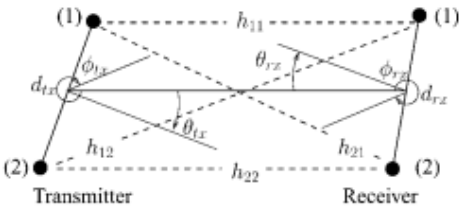

Figure 3.2 Illustration of path and antenna parameters in the azimuth plane for T_x and R_x terminals [42].

carrier frequency f_c. For f_c= 2 GHz, which is the frequency at which the empirical measurements were made for the SCM. The antenna orientation θ for the T_x and the R_x is defined with respect to the line-of-sight (LOS) path between the two terminals. The range of values for the array orientation is $0^0 \leq \theta \leq 90^0$. The angle of the ray arriving at or leaving from a terminal is denoted by Ø with the appropriate subscript, and is referenced to the LOS path. The ray angle ranges from $0^0 \leq Ø \leq 360^0$. We note, however, that based on the channel measurements, $Ø>180^0$ is seldom observed. The angle spread depends on the ray arrival/departure distribution and its power distribution and gives a measure of the scattering richness of the environment. The symbols h_{ij}, i = {1,2}, j = {1, 2} in Fig. 3.2 correspond to the path connecting the i_{th} receive antenna to the j_{th} transmit antenna, and they are elements of the channel matrix H [42].

3.3.2 Effects of array orientation and angle spread

The azimuth plane of a linear antenna array is shown in Fig. 3.3 and corresponds to the xy-axis. The z-axis is perpendicular to the diagram. The antenna array is orientated at an angle of θ with respect to the LOS path to the transmitter. The ray A shows the direction of propagation of a plane wave in the azimuth dimension. It impinges on the array elements with an angle of Ø / 2 with respect to the LOS path and has a normalised amplitude of $1/\sqrt{2}$. Ray B is identical to ray A except that it impinges on the array at an angle of –Ø / 2 with respect to the LOS path.

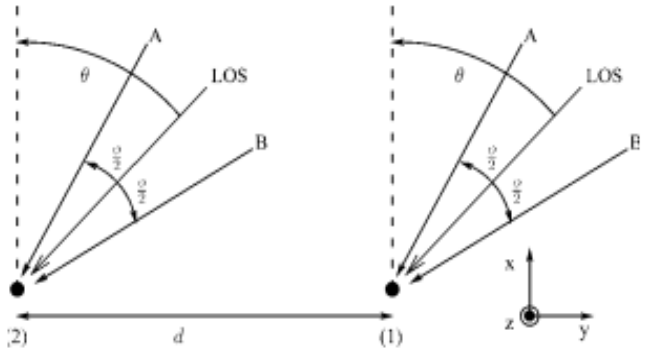

Figure 3.3 Physical geometry of the azimuth plane of a linear array in a static environment [42].

$$\mathbb{R} = \frac{1}{2}\left(1 + \cos\left(\frac{2\pi d}{\lambda}.2sin\frac{\emptyset}{2}cos\theta\right)\right)$$

$$= \frac{1}{2}\left(1 + \cos\left(\frac{4\pi}{\lambda}.d.\Delta\right)\right) \quad (3.3)$$

Where (.) is the complex conjugate operation, $\mathbb{R}$ denotes the real component of the quantity and $\Delta = sin\frac{\emptyset}{2}cos\theta$. In (3.3) we interpret Δ as scaling the element distance d. For $0^0 \leq \theta \leq 90^0$ and $0^0 \leq \emptyset \leq 180^0$, the cosine and sine terms of Δ range between zero and unity. The smaller the θ and the larger the Ø, the larger the term (d. Δ), which reduces the inner product. We interpret (d. Δ), as the effective distance between two antenna elements. The inner product and the correlation operation have the same dependencies on the variables Ø, or Ø, and θ. From (3.3), we conclude that the correlation will also depend on the effective distance (d. Δ) in the same way as for the inner product case. We therefore argue that a prediction of link performance based on path correlation behaviour is possible using (3.3). Specifically, increasing Ø will decrease the correlation, and increasing θ, will increase the correlation. The limitation of the inner product approach is that it does not consider the statistical distribution of Ø, which does affect the path correlation [42].

3.3.3 Mutual coupling (C_{mc})

An antenna is used to convert an electromagnetic field into induced voltage to be measured. However, when antenna elements are placed close to each other, the voltage at

each antenna can affect other antennas which are nearby. This is called mutual coupling. Mutual coupling depends on the distance between two dipoles d, the dipole length l, the thickness of wire t, dipole orientation and geometry. In order to model the effects of mutual coupling, the coupling matrix is introduced to characterize the mutual coupling properties at both transmitter and receiver. By using fundamental electromagnetic and circuit theory, the coupling matrix C of the antenna array is defined as

$$C_{mc}=((Z_A + Z_T)(\mathbf{Z} + Z_T \mathbf{I}_N))^{-1} \quad (3.4)$$

where Z_A is the antenna's impedance in isolation (for $l = \lambda/2$ dipole, $Z_A = 73 + j42.5\ \Omega$), $\mathbf{I}_N$ is the identity matrix, Z_T is the impedance of the receiver at each antenna element, chosen as the complex conjugate of Z_A to obtain an impedance match for maximum power transfer, and $\mathbf{Z}$ is the N ×N mutual impedance matrix which is given by

$$Z = \begin{pmatrix} Z_A & Z_{12} & \cdots & Z_{1n} \\ z_{21} & Z_A & \cdots & Z_{2n} \\ \vdots & \vdots & & \vdots \\ Z_{n1} & Z_{n2} & \cdots & Z_A \end{pmatrix} \quad (3.5)$$

3.4 MIMO Channel Model

In wireless communication, the transmitted signal is assumed to be received after a complicated propagation process, which may include scattering, refraction, reflection, and diffraction caused by the objects present in the communication scenario. Due to difficulties, an appropriate channel model is crucial for MIMO system capacity analysis. These models are discussed in detail below.

3.4.1 i.i.d. Channel Model

The independent and identically distributed (i.i.d.) flat Rayleigh fading channel is the simplest and the most common channel model. An i.i.d. flat Rayleigh fading MIMO channel is defined as

$$h_{mn} = \mathcal{N}(0,1/\sqrt{2}) + j\,\mathcal{N}(0, 1/\sqrt{2}) \quad (3.6)$$

Where hmn represents the complex gains between the n^{th} transmit and m^{th} receive antennas, $\mathcal{N}(0,1/\sqrt{2})$ is the normal distribution with zero mean and $(1/\sqrt{2})$ standard deviation.

In the i.i.d. case, antenna elements are assumed to be placed far from each other (at least more than 0.5 λ [8]) to ensure there are no spatial correlation and mutual coupling effects. In [2], the i.i.d channel also called spatially white channel (denoted by $\mathbf{H_w}$). Some properties of **Hw** are summarized:

$$\mathbf{E}\{[H_w]_{i,j}\} = 0,$$

$$\mathbf{E}\{|[H_w]_{i,j}|^2\} = 1,$$

$$\mathbf{E}\{[H_w]_{i,j}\,[Hw]^{\dagger}_{m,n}\} = 0.\ \text{If } I \neq m \text{ or } j \neq n; \tag{3.7}$$

where E{x} is the expectation of x and $[.]^{\dagger}$ is the complex conjugate transpose.

3.4.2 One-Ring Channel Model

The 'One-Ring' channel model has been described in [17,33]. In this model, the base station (BS) is assumed to be elevated, which means that there is no obstruction by local scattering while the mobile station (MS) is surrounded by scatterers lying in a circular disc with uniform distribution.

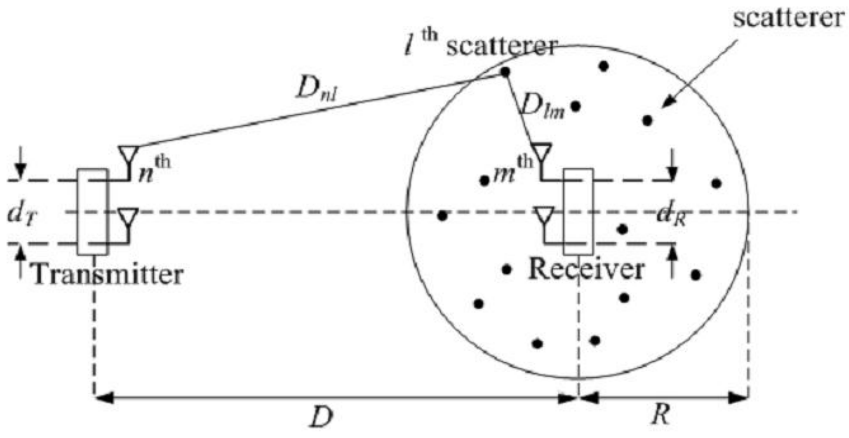

Figure 3.3 Illustration of the 'One-Ring' channel model.

The scatterers are assumed to be omnidirectional reradiating objects to reflect the plane wave directly to the receiver antenna without influencing other scatterers [17]. Only those rays that reflect once by the scatterer are considered. The geometrical description is shown in Figure 3.3. L scatterers are assumed to be uniformly distributed on a disc of radius R which is around the receiver. Usually R is assumed smaller compared with D, which is the distance between the transmitter and receiver. Furthermore, both R and D are assumed to be large compared with the antenna space dR and dT ({D > R}>> max(d_R, d_T)) [15]. Based on this model, the entries of the channel matrix in Equation (3.2) are generated as follows. Considering a single transmission path from n^{th} transmit antenna to m^{th} receive antenna intercepted and reflected by l^{th} scatterer, the channel gain h_{mn} is given as [12]

$$h_{mn} = \sqrt{1/L} \sum_{l=1}^{L} \alpha_l \exp[-j(2\pi/\lambda)(D_{nl} + D_{lm})] \qquad (3.8)$$

where α_l is the scattering coefficient from the l^{th} scatterer (l = 1, 2,...., L) and is modeled as a normal complex random variable with zero mean and unit variance, D_{lm} is the distance between the m^{th} receive antenna and l^{th} scatterer, D_{nl} is the distance between the 1^{th} scatterer and the n^{th} transmit antenna.

3.4.3 Spatial Channel Model

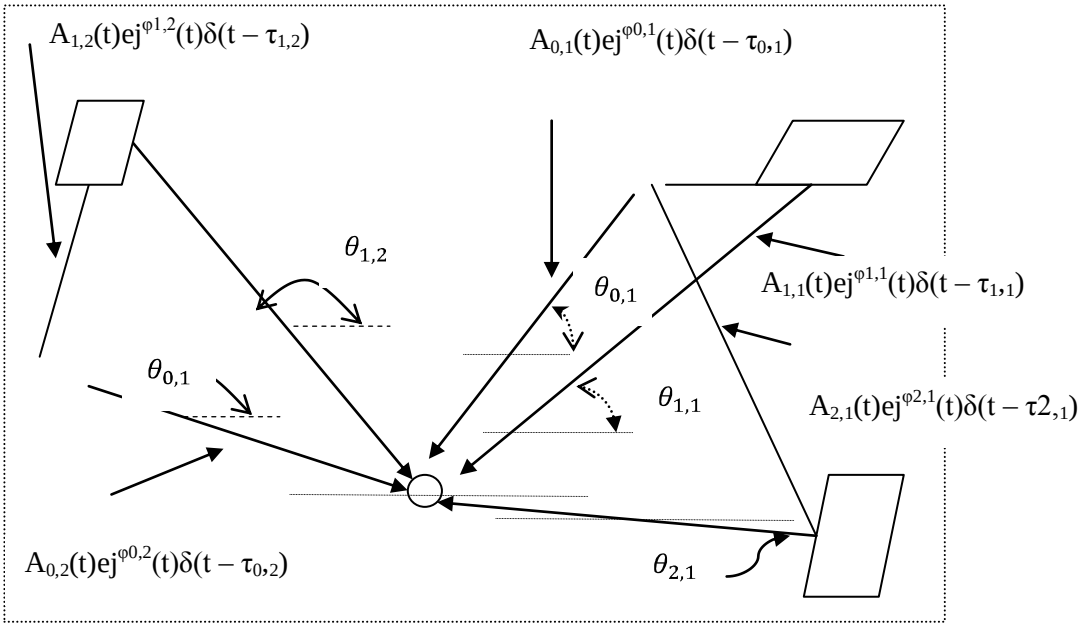

Figure 3.4 The multipath environment with two mobile stations.

The spatial channel model (SCM) is a standardized model established by combining the 3GPP-3GPP2 spatial channel model (SCM) with the adhoc group (AHG). Its scope is to develop and specify parameters and methods under spatial channel modeling for system and link level evaluations [18]. SCM is a 2-D parameter channel model, which considers N clusters of scatterers. Each cluster corresponds to a path. There are M un-resolvable sub paths with in a path (M = 20 for SCM) [21].

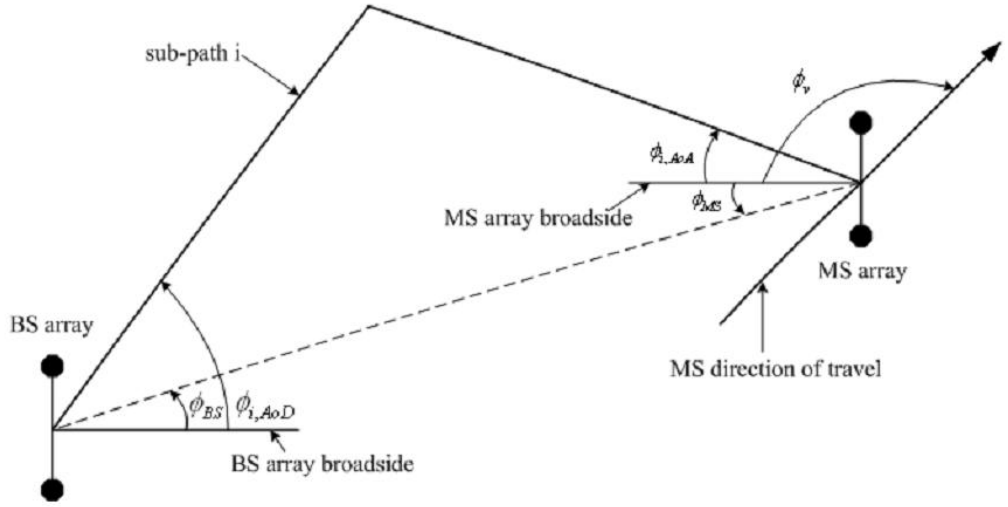

Figure 3.5: A simplified diagram of SCM for a 2 × 2 MIMO system [18].

A simplified pictorial of the multipath environment with two mobile stations is shown in Fig. 3.4. Each signal component experiences a different path environment, which will determine the amplitude A_{lk}, carrier phase shift φ_{lk}, time delay τ_{lk}, AOA θ_{lk} and Doppler shift f_d of the l^{th} signal component of the k^{th} mobile. In general, each of these signal parameters will be time-varying. Using this model, we can simulate urban micro cell and macro cell, as well as sub urban macro cell environments. In this model, both physical parameters and evaluation methodology have been considered [35].

Table 3.1: Angular parameter of a simplified SCM MODEL

Φ_{BS}	LOS AoD direction between the BS and MS, with respect to the broadside of the BS array.

Φ_{MS}	Angel between the BS-MS LOS and the MS broadside.
$\Phi_{i,AoD}$	Absolute AoD for the i^{th} (i=1…….M) sub-path at the BS, with respect to the BS broadside.
$\Phi_{i,AoA}$	Absolute AoA for the i^{th} (i=1…….M) sub-path at the MS, with respect to the BS broadside.
Φ_{v}	Angle of the velocity vector, with respect to the MS broadside.

3.5 Capacity analysis of various systems

C.Shannon first derived the channel capacity for additive white Gaussian noise (AWGN) channels in 1948 [36]. Compared with the scalar AWGN channels, a MIMO system can offer significant improvement to either communication quality (bit-error rate or BER) or transmission date rate (bits/sec) by exploiting spatial diversity [4]. We summarize absolute capacity bounds, which compare SISO, single-input-multiple-output (SIMO) and multiple- input-single-output (MISO) capacities. Since feedback is an important consideration of communication system designs. Before discussing capacity, some assumptions need to be stated:

- In all these cases, i focus on the single user form of capacity, so that the received signal is corrupted by additive white Gaussian noise only.
- Capacity analysis is based on a "quasi-static" situation which means that the channel is assumed fixed within a period of time (a burst), and the burst is assumed to be a long enough duration in which sufficient bits are transmitted to make information theory be meaningful [4, 8].
- The channels are assumed to be memoryless channels which mean that each channel realization is independent of the others [6].

3.5.1 SISO System Capacity

For a memory less SISO (single input single output) system the capacity is given by

$$C_{SISO} = \log_2(1 + \rho |h|^2) \text{ bps/Hz} \quad (3.9)$$

where ρ is the SNR at receiver antenna, and *h* is the normalized complex gain of the channel

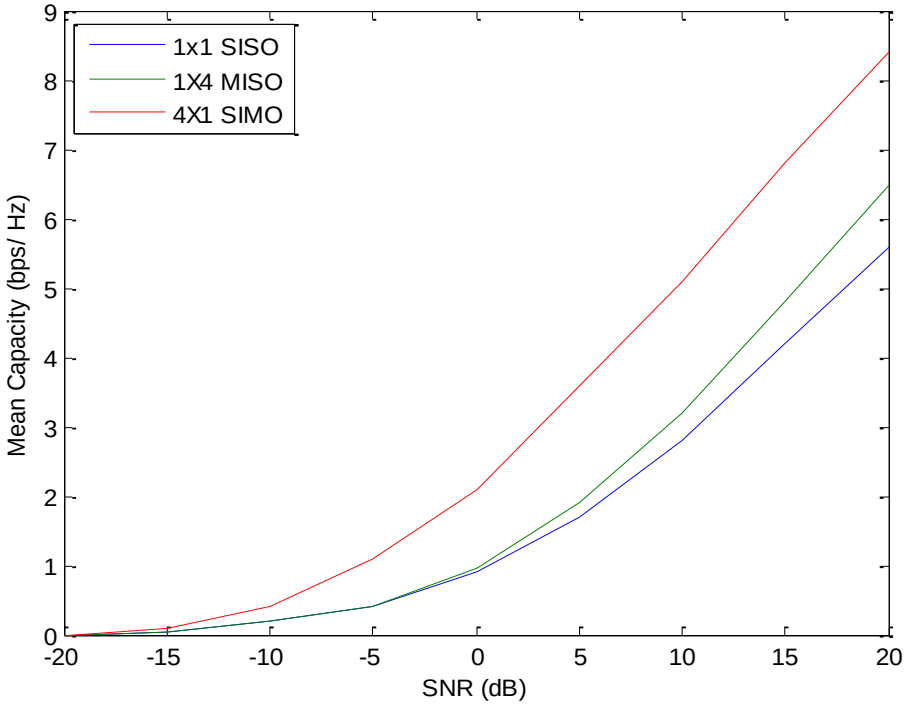

Fig.3.6: Comparison of mean capacity of SISO, SIMO and MISO systems as a function of SNR.

3.5.2 SIMO and MISO System Capacity

With N_R R_X antennas, the single-input-multiple-output (SIMO) system capacity is

$$C_{SIMO} = \log_2 (1+ \rho \sum_{m=1}^{N_R} |h_m|^2) \quad (3.10)$$

where h_m is the gain for m^{th} RX antenna. However, if $N_T T_x$ antennas are used, a multiple input single input (MIMO) is achieved. The capacity is given [4]

$$C_{SIMO} = \log_2 (1+ \frac{}{N_T} \sum_{m=1}^{N_R} |h_n|^2) \quad (3.11)$$

where h_n is the gain for n^{th} T_X antenna. In order to ensure transmitter power restriction, SNR is normalized by N_T. Figure 3.6 illustrates the capacity comparison of SISO, SIMO and MISO system versus SNR using Equation (3.9) - Equation (3.11). From the figure, we can see that the SIMO and MISO channels improve the capacity compared with the SISO channel by exploiting more antennas. However, the SIMO and

MISO channels can only offer a logarithmic increase in capacity with the number of antennas [2]. Comparing Equation (3.10) and (3.11) it is clear that $C_{\text{MISO}} < C_{\text{SIMO}}$ when the channel information is not available at the transmitter [2].

3.5.3 MIMO System Capacity with Equal Power

For N_T T_X and N_R R_X antennas, the equal power capacity is equation is [6, 8]

$$C_{EP} = \log_2 [\det(1+\frac{}{N_t} HH^{\dagger})] \quad \text{bps/Hz} \tag{3.12}$$

where det (·) denotes the determinant of a matrix, **I** is an $N_R \times N_T$ identity matrix, ρ is the average received Signal to Noise Ratio (SNR), and $\mathbf{H}^{\dagger}$ is the complex conjugate transpose of **H**. In order to investigate the characteristics of **H**, we can perform singular value decomposition (SVD) of **H** to diagonalize **H** and find the eigenvalues. An SVD expansion of any matrix $\mathbf{H}(N_R \times N_T)$ can be written as [6]

$$\mathbf{H} = \mathbf{UDV}^{\dagger} \tag{3.13}$$

Where $\mathbf{U}$ $(N_R \times N_R)$ and $\mathbf{V}$ $(N_T \times N_T)$ are unitary matrices, which means that

$$\mathbf{UU}^{\dagger} = \mathbf{VV} = \mathbf{I}. \mathbf{D}$$

$(N_R \times N_T)$ is non-negative and diagonal with entries specified by

$$D = \text{diag}(\sqrt{\lambda_1}, \sqrt{\lambda_2}, \ldots \ldots \sqrt{\lambda_{m,}}, 0, \ldots \ldots, 0) \tag{3.14}$$

where diag (A) is the vector consisting of the diagonal elements of A, $_1, _2, . . m$ are the nonzero eigenvalues of **W**, $m = \min(N_R, N_T)$, and

$$W = \begin{cases} HH^{\dagger}, & N_R \leq N_T \\ H^{\dagger}H, & N_T < N_R \end{cases} \tag{3.15}$$

The columns of **U** are the eigenvectors of $\mathbf{HH}^{\dagger}$ and the columns of **V** are the eigenvectors of $\mathbf{H}^{\dagger}\mathbf{H}$ [6]. This SVD (Equation (3.13)) shows that the channel matrix **H** can be diagonalized to a number of independent orthogonal subchannels, where the power gains of the i^{th} channel is λ_i [4].

3.5.4 MIMO System Capacity with Waterfilling

When the channel knowledge is absent at the transmitter, the individual subchannels are not accessible. So that equal power allocation is logical under this scenario. When the transmitter has perfect knowledge of the channel, the waterfilling method is used to optimize the transmitted signal power scheme [13].

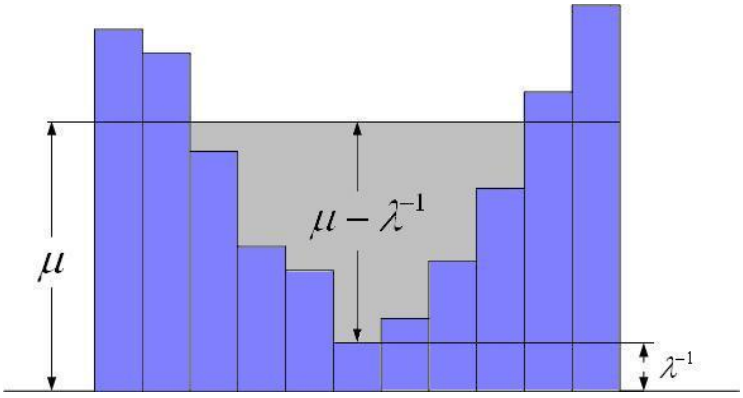

Figure 3.7: Illustration of Waterfilling.

The principle of the Waterfilling theorem sees the division of total power in such a way that a greater portion goes to the channels with higher gain and less or evens none to the channels with small gains. The solution is given below [6, 13]

$$C_{WF} = \sum_{i=1}^{m} log_2(\mu\lambda_i)^+ \text{ bps/Hz} \quad (3.16)$$

where μ is chosen from the waterfilling algorithm, which is

$$= \sum_{i=1}^{m} (\mu - \lambda_i)^+ \quad (3.17)$$

where (.)+ denotes taking only those terms which are positive and λ_1, ……,λ_m are the eigenvalues of W with m = min(N_T, N_R). Compared with the equal power scheme, waterfilling has a significant advantage especially at low SNR. However, this advantage decreases as SNR is increased [13].

3.6 MIMO System Performance Measures

The MIMO system capacity is compared in terms of the following performance measures.

3.6.1 Mean and Outage Capacity

Since the channel H is random, the capacity of the MIMO channel is a random variable. The capacity of fading channels can be defined in a number of ways. In practice, mean capacity and outage capacity are the two most commonly used statistical measures. The mean capacity $\overline{C}$ of a MIMO channel is the ensemble average of the information rate over the all realizations of the channel matrix H [2]. The mean capacity is given by [2, 6]

$$\overline{C} = E\left\{\sum_{i=1}^{m} \log_2\left(1 + \frac{}{N_T}\lambda_i\right)\right. \text{ bps/Hz} \qquad (3.18)$$

The outage capacity defines the level of capacity that is guaranteed with a certain level of reliability, and we can define the q% outage capacity Cout, q as the information rate that is guaranteed for (100 - q)% of the channel realization, i.e. [2]

$$P(C \leq C_{out,q}) = q\% \qquad (3.19)$$

The significance of the mean capacity is that in an ergodic channel, we can transmit the signal at the rate given by mean capacity without errors. In this sense, the mean capacity is the right metric when the channel is known to the transmitter. Outage capacity is a useful characterization when the channel is unknown to the transmitter and H is random but held constant for each use of the channel [2]. Here, mean capacity is used as performance measure. This is done to enable comparison between waterfilling and equal power results.

3.7 Fading

Most mobile communication systems are used in and around center of population. The transmitting antenna or Base Station (BS) are located on top of a tall building or tower and they radiate at the maximum allowed power. In the other hand, the mobile antenna or Mobile Station (MS) is well below the surrounding buildings. Consequently, the radio channel is influenced by the surrounding structures such as cars, buildings etc. The wireless channel can be described as a function of time and space and the received signal is the combination of many replicas of the original signal impinging at receiver (R_X) from many different paths The signal on these different paths can constructively or

destructively interfere with each other. This is referred as multipath. If either the transmitter or the receiver is moving, then this propagation phenomena will be time varying, and fading occurs. In addition to propagation impairments, the other phenomena that limit wireless communications are noise and interference. It is interesting to notice that wireless communication phenomena are mainly due to scattering of electromagnetic waves from surfaces or diffraction, e.g. over and around buildings. The design goal is to make the received power adequate to overcome background noise over each link, while minimizing interference to other more distant links operating at the same frequency. Fading is of two types:

1. Large Scale Fading
2. Small Scale Fading
3. Large Scale Fading

Small scale fading models that have widely used for modeling the fading environment are:

- Rayleigh fading
- Rician fading
- Nakagami fading

3.8 Summary

This chapter has described the system model for MIMO systems. The MIMO channel models (the 'One-Ring' and SCM channel model), fading have been described in detail. The formulas of MIMO system capacity with equal power and waterfilling have been summarized, after discussion of SISO, SIMO and MISO system capacity

Chapter 4

MIMO System Performance based on Spatial Channel Model

In this chapter, the simulation results are described. The simulation was done on MATLAB R2007b (7.5) software. We have done a comparative study of channel capacity of spatial channel model, investigate the performance of channel capacity variation with time, variation in spatial autocorrelation with time and generate its power delay profile.

4.1 SCM Parameter Assumptions

SCM offers three simulation environments: suburban macro-cell, urban macro-cell and urban micro-cell.

Suburban Macro: The suburban macro cell scenario describes a rural/suburban area with generally residential buildings and structures. The vegetation and any hills in the area are also assumed not to be too high. The BS antenna position is high, well above local clutter. As a result, the AS and DS are relatively small. In addition, the base-to-base distance is approximately 3 km.

Urban Macro: The urban macro cellular environment describes large cells in areas with urban buildings of moderate heights in the vicinity and significant scattering. The BS antennas are placed at high elevations, well above the rooftops of any buildings in the immediate vicinity. The distance between BSs is again about 3km. This scenario assumes moderate to high ASs at the BS and also large DSs. In urban environments, street canyon effects, i.e., wave propagation down relatively narrow streets with high buildings on both sides may be important in some cases and depending on their probability of occurrence, may lead to deviations from the generic urban macro cell case. Thus, street canyon effects are treated as optional extensions to the urban macro scenario. Another important effect, also treated as an option in this scenario, is the existence of additional clusters of energy due to far scatterers originating from high buildings.

Urban Micro: The urban micro cell scenario describes small urban cells with inter base distances of approximately 1km. Base antennas are located at roof top level and therefore large ASs are expected at the BS, even though the DS is only moderate.

In the case of macro cell scenarios discussed above, due to the relatively large area allocated to each BS, the fraction of locations in the cell with the chance to have a line-of-sight (LOS) component from the BS is small. Thus, for simplicity such channels are not modelled in the macro cell cases. However, for smaller cells, as in the case of micro cell scenario, the users with LOS components cannot always be neglected.

4.2 Spatial channel model for simulations

The spatial channel model for use in the system-level simulations is described here. As in the link level simulations, the description is in the context of a downlink system where the BS transmits to a MS. As opposed to link simulations which simply consider a single BS transmitting to a single MS, the system simulations typically consist of multiple cells/sectors, BSs, and MSs. Performance metrics such as throughput and delay are collected over D drops, where a "drop" is defined as a simulation run for a given number of cells/sectors, BSs, and MSs, over a specified number of frames. During a drop, the channel undergoes fast fading according to the motion of the MSs. Channel state information is fed back from the MSs to the BSs, and the BSs use schedulers to determine which user(s) to transmit to. Typically, over a series of D drops, the cell layout and locations of the BSs are fixed, but the locations of the MSs are randomly varied at the beginning of each drop. To simplify the simulation, only a subset of BSs will actually be simulated while the remaining BSs are assumed to transmit with full power. For an S element BS array and a U element MS array, the channel coefficients for one of N multipath components are given by an S -by- U matrix of complex amplitudes.

4.2.1 General parameters and assumptions

The received signal at the MS consists of N time-delayed multipath replicas of the transmitted signal. These N paths are defined by powers and delays and are chosen

randomly according to the channel generation procedure. Each path consists of M sub paths.

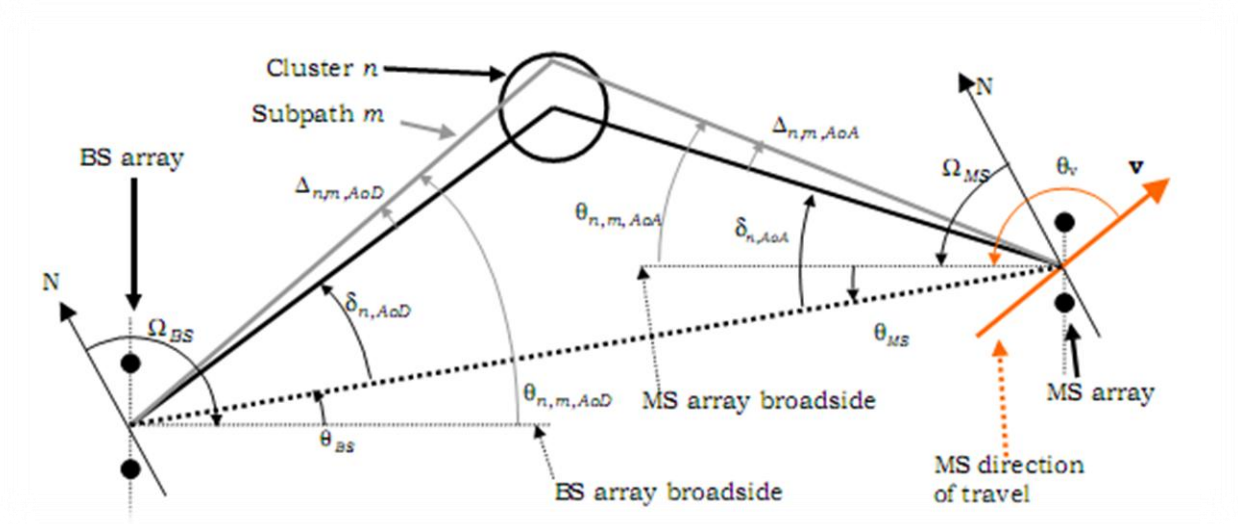

Figure 4.1: Angular variable definitions [18]

The angles shown in Figure 4.1 that are measured in a clockwise direction are assumed to be negative in value.

Table 4.1: BS and MS angle parameters

Ω_{BS}	BS antenna array orientation, defined as the difference between the broadside of the BS array and the absolute North (N) reference direction.
θ_{BS}	LOS AoD direction between the BS and MS, with respect to the broadside of the BS array.
$\delta_{n,\,AoD}$	AoD for the nth (n = 1 … N) path with respect to the LOS AoD $^{\theta 0.}$
$\Delta_{n,m,\,AoD}$	Offset for the mth (m = 1 … M) subpath of the nth path with respect to $^{\delta n,\,AoD}$
$\theta_{n,m,\,AoD}$	Absolute AoD for the mth (m = 1 … M) subpath of the nth path at the BS with respect to the BS broadside.

Ω_{MS}	MS antenna array orientation, defined as the difference between the broadside of the MS array and the absolute North reference direction
θ_{MS}	Angle between the BS-MS LOS and the MS broadside.
$\delta_{n, AoA}$	AoA for the nth (n = 1 … N) path with respect to the LOS AoA $\theta_{0,MS}$
$\Delta_{n,m, AoA}$	Offset for the m_{th} (m = 1 … M) subpath of the nth path with respect to $\delta^{n,AoA.}$
$\theta_{n,m, AoA}$	Absolute AoA for the mth (m = 1 … M) sub path of the nth path at the MS with respect to the BS broadside.
v	MS velocity vector.
θ_v	Angle of the velocity vector with respect to the MS broadside: θv = arg(v).

For system level simulation purposes, the fast fading per-path will be evolved in time, although bulk parameters including angle spread, delay spread, log normal shadowing, and MS location will remain fixed during the its evaluation during a drop.

Table 4.2 Environment parameters

Parameters	
No. of antennas of BS array	2
No. of antennas of MS array	2
Distance between neighboring elements at BS array in wavelengths	6
S per path angle spread in degrees	35

Carrier frequency in GHz	2
MS velocity in km/h	60

The following are general assumptions made for all simulations, independent of environment:

a) Uplink-Downlink Reciprocity: The AoD/AoA values are identical between the uplink and downlink.
b) For FDD systems, random sub path phases between UL, DL are uncorrelated. (For TDD systems, the phases will be fully correlated.) Shadowing among different mobiles is uncorrelated. In practice, this assumption would not hold if mobiles are very close to each other, but we make this assumption just to simplify the model.
c) The spatial channel model should allow any type of antenna configuration (e.g. whose size is smaller than the shadowing coherence distance) to be selected, although details of a given configuration must be shared to allow others to reproduce the model and verify the results. It is intended that the spatial channel model be capable of operating on any given antenna array configuration. In order to compare algorithms, reference antenna configurations based on uniform linear array configurations with 0.5, 4, and 10 wavelength inter-element spacing will be used.
d) The composite AS (angle spread), DS (delay spread), and SF (shadow fading), which may be correlated parameters depending on the channel scenario, are applied to all the sectors or antennas of a given base. Sub-path phases are random between sectors. The AS is composed of 6 x 20 sub-paths, and each has a precise angle of departure which corresponds to an antenna gain from each BS antenna. The effect of the antennas gain may cause some change to the channel model in both AS and DS between different base antennas, but this is separate from the

channel model. The SF is a bulk parameter and is common among all the BS antennas or sectors.

e) To allow comparisons of different antenna scenarios, the transmit power of a single antenna case shall be the same as the total transmit power of a multiple antenna case

f) The generation of the channel coefficients assumes linear arrays. The procedure can be generalized for other array configurations.

4.3 Result

4.3.1 Mean Capacity vs. Number of Antenna

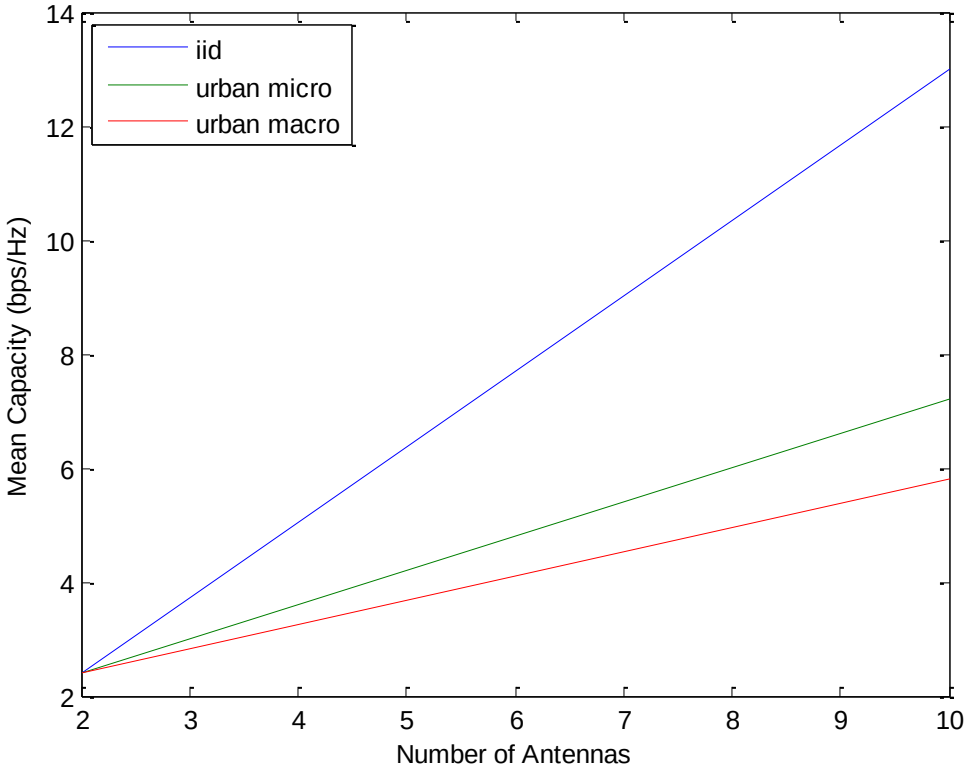

Fig 4.2 Capacity vs. No of antenna

Figure 4.2 show the mean capacity as a function of the number of antennas ($N_T = N_R$) for $\rho = 3$ dB, $dT = dR = 0.5\ \lambda$, assuming equal power and waterfilling schemes. We can see that for the SCM channel the capacity does not double by doubling the number of antennas, when the number of antennas double from 2 to 4, the suburban macro cell capacity increases from about 2.33 bps/Hz to 3.28 bps/Hz, i.e. an increase of about 40%, while the urban microcell capacity increases by about 51%. These simulation results show that SCM model gives a more realistic assessment of MIMO capacity.

4.3.2 Channel fast fading

A. For Suburban Macrocell Environment,

for d = 157

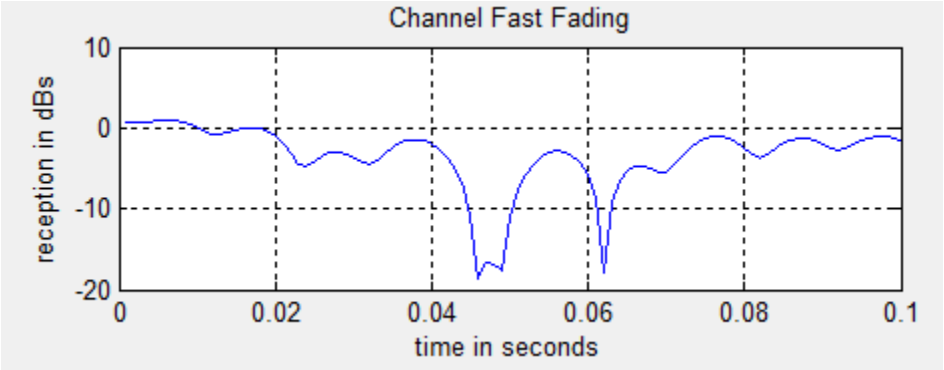

Figure 4.3: Channel fast fading for suburban macrocell for d= 157.

for d = 733

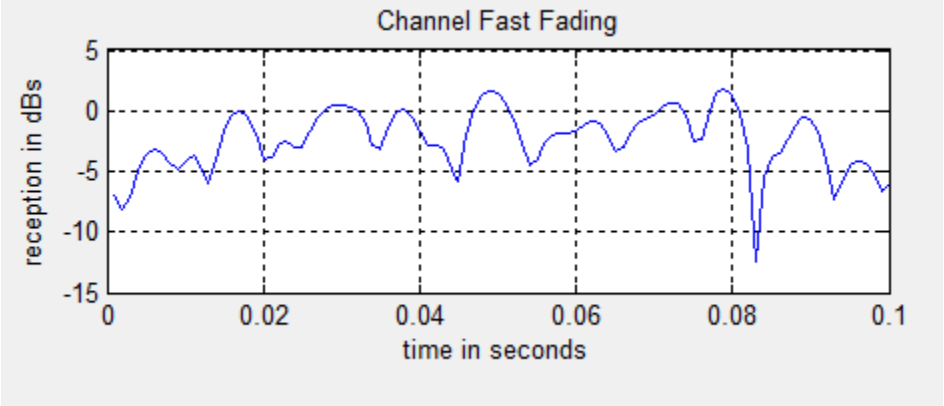

Figure 4.4: Channel fast fading for Suburban Macrocell for d= 733.

B. Urban Macrocell Environment

for d = 12

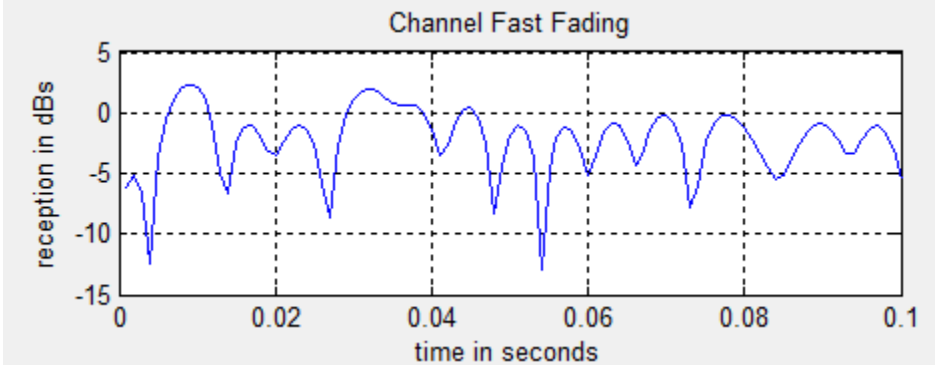

Figure 4.5: Channel fast fading for Urban Macrocell for d= 12.

for d = 356

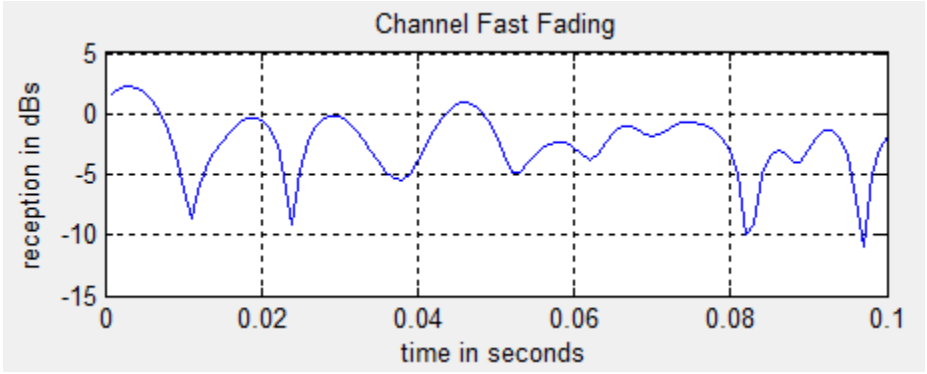

Figure 4.6: Channel fast fading for Urban Macrocell for d= 356

C. Urban Microcell Environment

for d = 3

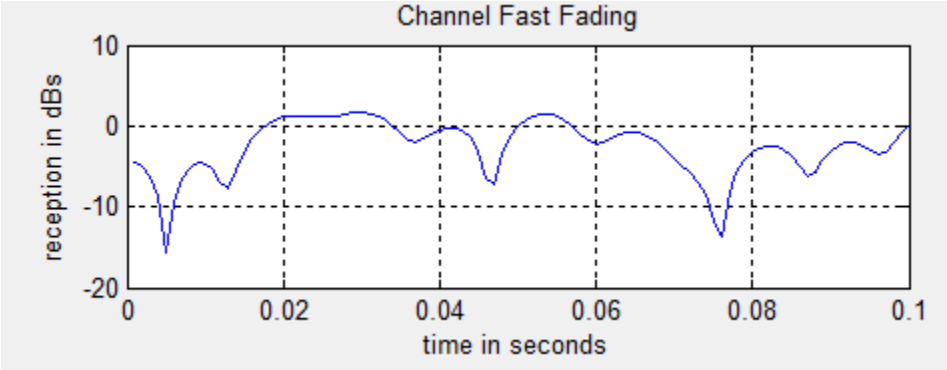

Figure 4.7: Channel fast fading for Urban Microcell for d= 3.

for d = 188

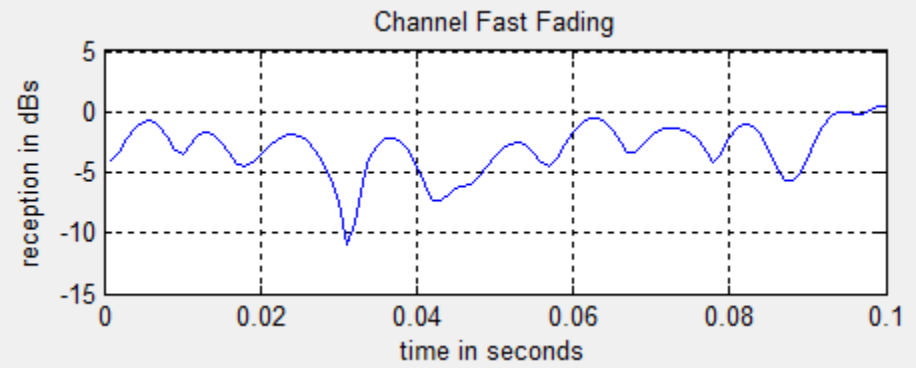

Figure 4.8: Channel fast fading for Urban Microcell for d= 188.

From the above results it is concluded that with increasing the distance between BS and MS, the received signal strength decreases due to fast fading.

4.3.3 Channel Capacity

A. For Suburban Macrocell Environment

for d = 157

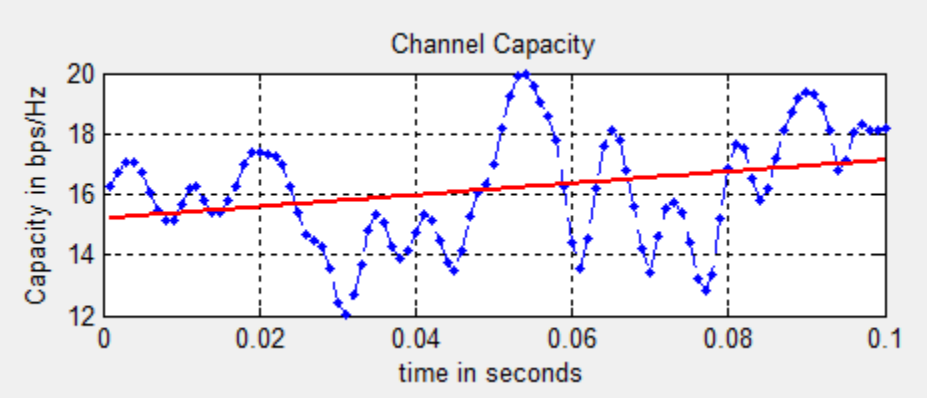

Figure 4.9: Channel Capacity for Suburban Macrocell for d= 157.

B. Urban Macrocell Environment

for d = 134

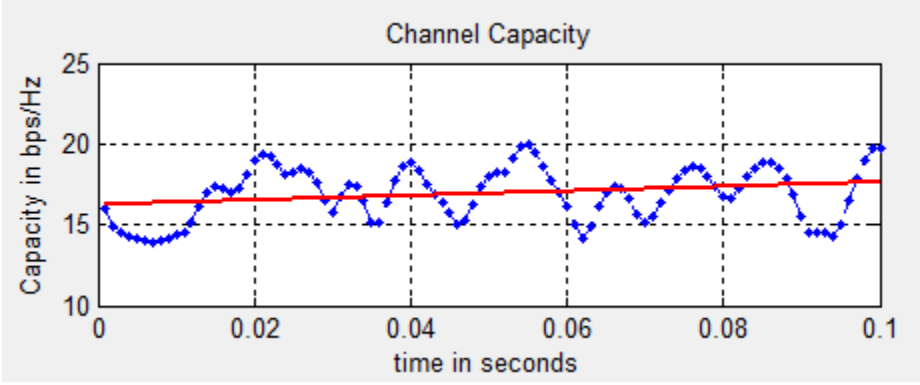

Figure 4.10: Channel Capacity for Urban Macrocell for d= 134.

C. Urban Microcell Environment

for d = 188

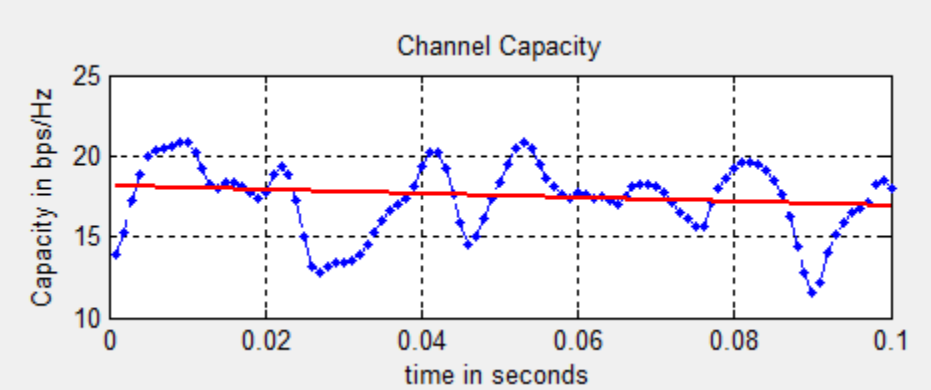

Figure 4.11: Channel Capacity for Urban Microcell for d= 188.

The variation in channel capacity with time for suburban macrocell, urban macrocell and urban micro cell environments have shown here.

4.3.4 Spatial Autocorrelation

A. For Suburban Macrocell Environment

for d = 157

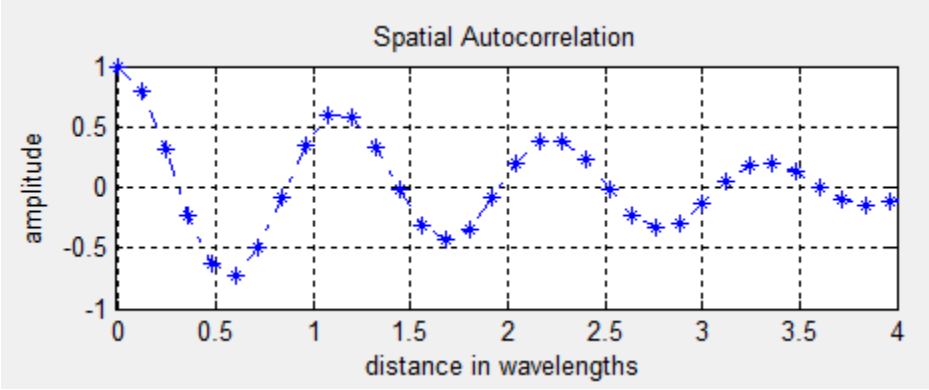

Figure 4.12: Spatial Autocorrelation for Suburban Macrocell for d= 157.

for d = 624

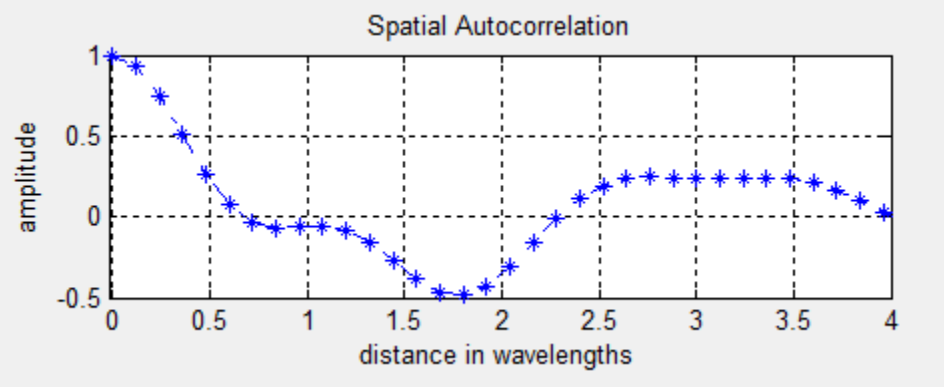

Figure 4.13: Spatial Autocorrelation for Suburban Macrocell for d= 624.

B. Urban Macrocell Environment,

for d = 12

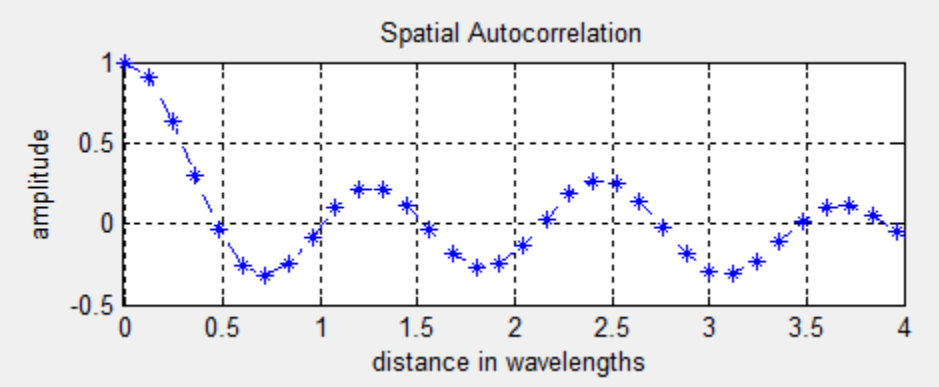

Figure 4.14: Spatial Autocorrelation for Urban Macrocell for d= 12.

for d = 134

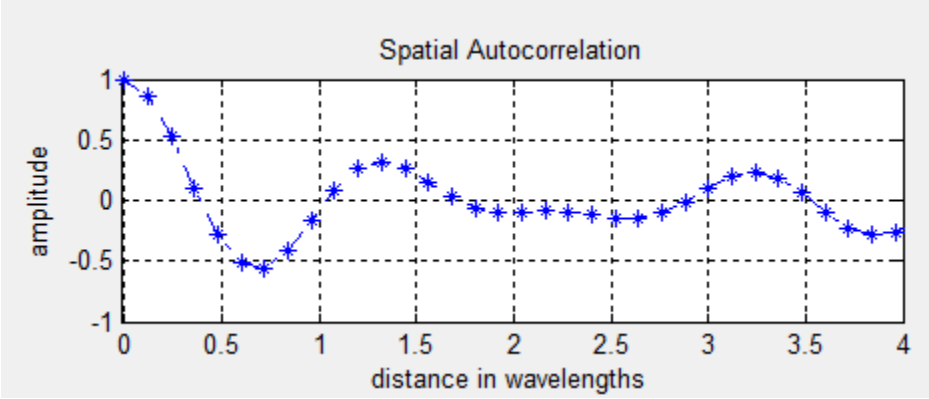

Figure 4.15: Spatial Autocorrelation for Urban Macrocell for d= 134.

C. Urban Microcell Environment

for d = 3

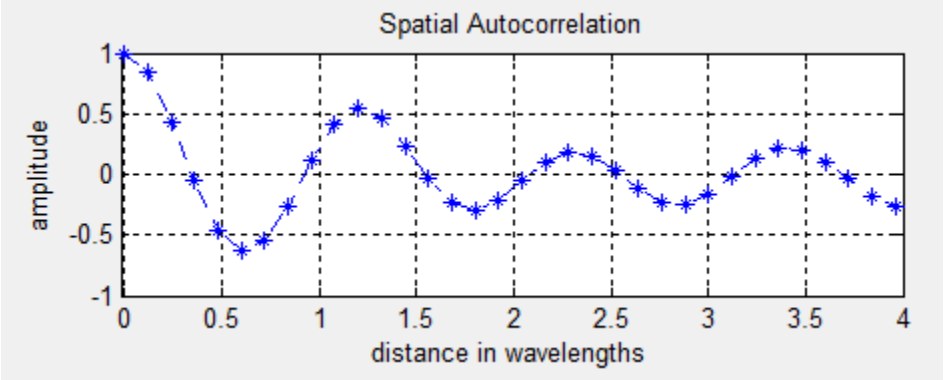

Figure 4.16: Spatial Autocorrelation for Urban Microcell for d= 3.

for d = 188

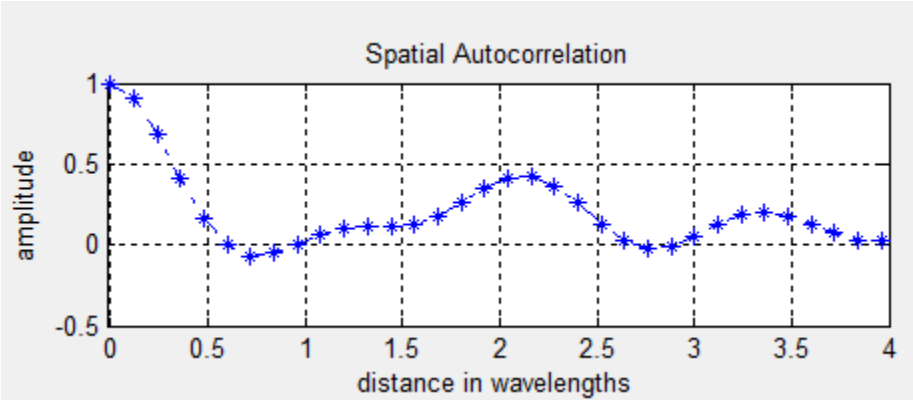

Figure 4.17: Spatial Autocorrelation for Urban Microcell for d= 188.

The amplitude in graph for Spatial Autocorrelation for suburban macrocell, urban macrocell and urban microcell environments is decreasing with the increase in the distance between BS and MS.

4.3.5 Power Delay Profile

A. For Suburban Macrocell Environment

for d = 157

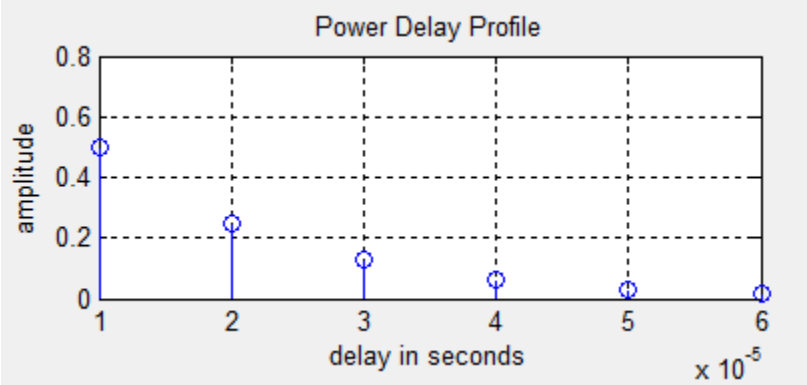

Figure 4.18: Power Delay Profile for Suburban Macrocell for d= 157.

B. Urban Macrocell Environment

for d = 134

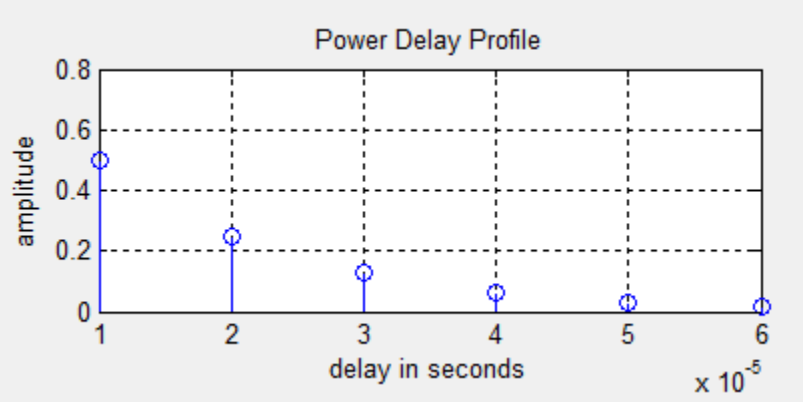

Figure 4.19: Power Delay Profile for Urban Macrocell for d= 134.

C. Urban Microcell Environment

for d = 188

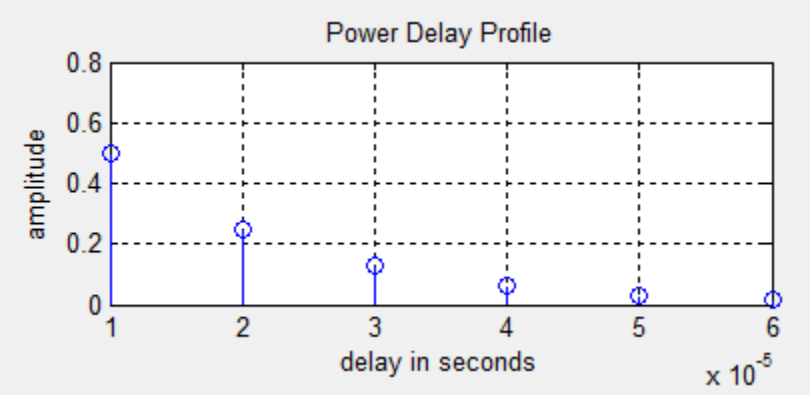

Figure 4.20: Power Delay Profile for Urban Microcell for d= 188.

The amplitude in graph for Power Delay Profile for suburban macrocell, urban macrocell and urban microcell environments is decreasing with the increase in the distance between BS and MS.

4.4 Summary

In this chapter, we have investigated MIMO system capacity using the Spatial Channel Model (SCM) and Channel Fast Fading, Channel Capacity, Spatial Autocorrelation, Power delay profile for different channel environments, proposed by standardization bodies (3GPP-3GPP2) for third generation systems. The mean capacity results of the SCM channel model as a function of number of antennas and SNR have been described. The capacities of suburban macrocell and urban microcell have been compared

Chapter 5

Conclusions and Future Work

5.1 Summary of Thesis Conclusions

In Chapter 3, a system model has been presented for investigating the capacity of MIMO systems. The i.i.d., 'One-Ring' and SCM channel models have been detailed. The basic capacity formulas for SISO, SIMO, MISO have been summarized. The coupling matrix approach has been discussed to model the effect of mutual coupling in MIMO systems

In Chapter 4, the performance of the channel for different propagation scenarios is investigated and the performance of the MIMO system has been investigated for different SCM propagation scenarios. The capacity of the urban microcell was found to be higher than the capacity of the suburban macrocell. This is because the increased angle spread in the urban microcell reduces correlation and increases capacity. It has been shown that the SCM capacity does not increase linearly with the number of antennas.

5.2 Future Work

Although this thesis has given valuable insights into MIMO capacity, there are many more issues that could be selected for further research and implementation in MIMO systems.

The number of paths used in Chapter 3 can be increased from 6 path with carrier frequency more than 5GHz.

References

[1] T. S. Rappaport, “Wireless Communications: Principles and Practice”, 2nd ed. Prentice Hall, 2002.

[2] A. Paulraj, R. Nabar, and D. Gore, “Introduction to Space- Time Wireless Communication”. Cambridge, New York, Cambridge University Press, 2005.

[3] E. Biglieri and G. Taricco, “Transmission and Reception with Multiple Antennas: Theoretical Foundations”, ser. Foundations and trends in communications and information theory. Hanover, MA, Now Publishers, 2004.

[4] D. Gesbert, M. Shafi, D. shan Shiu, P. J. Smith, and A. Naguib, “From theory to practice: an overview of MIMO space-time coded wireless systems,” IEEE J. Selected Areas Communication, vol. 21, no. 3, pp. 281–302, Apr. 2003.

[5] M. A. Jensen and J. W. Wallace, “A review of antennas and propagation for MIMO wireless systems,” IEEE Trans. Antennas Propagation, vol. 52, no. 11, pp. 2810–2824, Nov. 2004.

[6] I. E. Telatar, “Capacity of multi antenna gaussian channels,” Office for Official Pub- lications of the European Transactions on Telecommunications, Vol. 10, No. 6, pp. 585-595, Nov/Dec 1999.

[7] G. J. Foschini, “Layered space time architecture for wireless communication in a fading environment when using multi element antennas,” Bell Labs Technical Journal, pp. 41–59, 1996.

[8] G. J. Foschini and M. J. Gans, “On limits of wireless communications in a fading environment when using multiple antennas,” Wireless Pers. Comm., vol. 6, no. 3, pp. 311–335, Mar. 1998.

[9] H. N. M. Mbonjo, J. Hansen, and V. Hansen, “MIMO capacity and antenna array design,” proceeding Global Telecommunications Conference, IEEE, vol. 5, pp. 3155–3159, Nov. 2004.

[10] D.-S. Shiu, G. J. Foschini, M. J. Gans, and J. M. Kahn, “Fading correlation and its effect on the capacity of multielement antenna systems,” IEEE Trans. Commun.,

vol. 48,issue 3, pp. 502–513, Mar. 2000.

[11] B. O. Hogstad and M. Patzold, “Capacity studies of MIMO channel models based on the geometrical one-ring scattering model,” in Personal, Indoor and Mobile Radio Communications, 2004. 15th IEEE International Symposium on, vol. 3, no. 5-8, pp. 1613 – 1617, Sep. 2004.

[12] T. Svantesson and A. Ranheim, “Mutual coupling effects on the capacity of multiple antenna systems,” in Proc. IEEE ICASSP01, vol. 4, pp. 2485–2488, May 2001.

[13] P. J. Smith and M. Shafi, “Waterfilling methods for MIMO systems,” in 3rd Australian Communications Theory Workshop, Canberra, Australia, pp. 33–37, Feb. 4-5, 2002

[14] K. Yu and B. E. Ottersten, “Models for MIMO propagation channels: a review.” Wireless Communications and Mobile Computing, vol. 2, no. 7, pp. 653–666, 2002.

[15] M. Patzold and B. O. Hogstad, “A space-time channel simulator for MIMO channels based on the geometrical one-ring scattering model,” Vehicular Technology Conference, IEEE 60th, vol. 1, no. 26-29, pp.144–149, Sep. 2004.

[16] T. Svantesson, “A physical MIMO radio channel model for multi-element multi- polarized antenna systems,” in IEEE Vehicular Technology Conference, IEEE, vol. 2, pp. 1083–1087, 2001.

[17] P. Petrust, J. H. Reed, and T. S. Rappaport, “Geometrically based statistical channel model for macrocellular mobile environments,” in IEEE Global Telecommunications Conference, vol. 2, pp. 1197–1210, , Nov. 1996

[18] 3rd Generation Partnership Project (3GPP), “Spacial channel model for multiple input multiple output (MIMO) simulations (3gpp tr 25.996 version 6.1.0 release 6),” ETSI, Tech. Rep., 2003.

[19] B. K. Lau, S. M. S. Ow, G. Kristensson, and A. F. Molisch, “Capacity analysis for compact MIMO systems,” in Proc. IEEE VTC, vol. 1, pp. 165–170, June 2005.

[20] Gong, J.; Hayes, J.F.; Soleymani, M.R., “The effect of antenna physics on fading correlation and the capacity of multielement antenna systems”, proceeding electrical and computer engineering, 2005. Canadian Conference, pp. 1363-1366,

2005

[21] J. Salo, G. Del Galdo, J. Salmi, P. Kyosti, M. Milojevic, D. Laselva, and C. Schneider, “MATLAB implementation of the 3GPP Spatial Channel Model (3GPP TR 25.996),” On-line, Jan. 2005, http://www.tkk.fi/Units/Radio/scm/.

[22] B. Clerckx, D. Vanhoenacker Janvier, C. Oestges, and L. Vandendorpe, “Mutual coupling effects on the channel capacity and the space-time processing of MIMO com- munication systems,” in Proc. IEEE ICC, vol. 4, pp. 2638-2642, 2003.

[23] S. Durrani and M. E. Bialkowski, “Effect of mutual coupling on the interference re- jection capabilities of linear and circular arrays in CDMA systems,” IEEE Trans. An- tennas Propagat., vol. 52, no. 4, pp. 1130–1134, Apr. 2004.

[24] P. Fletcher, M. Dean, and A. Nix, “Mutual coupling in multielement array antennas and its influence on MIMO channel capacity,” Electronics Lett., vol. 39, no. 4, pp. 342–344, Feb. 2003.

[25] R. Janaswamy, “Effect of element mutual coupling on the capacity of fixed length linear arrays,” IEEE Antennas Wireless Propagat. Lett., vol. 1, pp. 157–160, Oct. 2002.

[26] V. Jungnickel, V. Pohl, and C. von Helmolt, “Capacity of MIMO systems with closely spaced antennas,” IEEE Commun. Lett., vol. 7, no. 8, pp. 361–363, Aug. 2003.

[27] P.-S. Kildal and K. Rosengren, “Correlation and capacity of MIMO systems and mutual coupling, radiation efficiency, and diversity gain of their antennas: simulations and measurements in a reverberation chamber,” IEEE Commun. Mag., vol. 42, pp.104–112, Dec. 2004.

[28] X. Li and Z.P. Nie, “Mutual coupling effects on the performance of MIMO wireless channels,” IEEE Antennas Wireless Propagat. Lett., vol. 3, pp. 344–347, Aug. 2004.

[29] M. K. Ozdemir, H. Arslan, and E. Arvas, “Mutual coupling effect in multi-antenna wireless communication systems,” in Proc. IEEE GLOBECOM03, vol. 2, pp. 829–833, Dec. 2003.

[30] J. W. Wallace and M. A. Jensen, “Mutual coupling in MIMO wireless systems: A rigorous network theory analysis,” IEEE Trans. Wireless Commun., vol. 3, no. 4,

pp. 1317–1325, July 2004.

[31] V. Pohl, V. Jungnickel, T. Haustein, and C. VonHelmolt, “Antenna spacing in MIMO indoor channels,” in Proc. IEEE VTC,2002, vol. 2, pp. 749–753.

[32] A. M. Wyglinski and S. D. Blostein, “On uplink CDMA cell capacity: mutual coupling and scattering effects on beamforming,” in IEEE Trans. Veh. Technol., vol. 52, no. 2, March 2003.

[33] R. B. Ertel, P. Cardieri, and K. W. Sowerby, “Overview of spatial channel models for antenna array communication systems,” Personal Commun. Mag., vol. 5, pp. 10–22, Feb. 1998.

[34] T. Svantesson, “Correlation and channel capacity of MIMO systems employing mul- timode antennas,” IEEE Trans. Veh. Technol., vol. 51, no. 6, pp. 1304–1312, Nov. 2002.

[35] M. Shafi, M. Zhang, A. L. Moustakas, P. J. Smith, A. F. Molisch, F. Tufvesson, and S. H. Simon, “Polarized MIMO channels in 3-d: models, measurements and mutual information,,” IEEE J. Select. Areas Commun., vol. 24, no. 3, pp. 514 – 527, March 2006.

[36] C. Shannon, “A mathematical theory of communication,” Bell Labs Technical Journal, vol. 27, pp. 379–423,623–656, July and October 1948.

[37] A. F. Molisch, “Effect of far scatterer clusters in MIMO outdoor channel models,” proceeding Vehicular Technology Conference, VTC 2003., vol. 1, pp.534–538.

[38] Cheng-Xiang Wang, Xuemin Hong, Hanguang Wu, and Wen Xu, “Spatial Temporal Correlation Properties of the 3GPP Spatial Channel Model and the Kronecker MIMO ChannelModel”, Hindawi Publishing Corporation, EURASIP Journal on Wireless Communications and Networking, Vol.2007, Issue 1, Pages: 59 –67. 2007

[39] R. Michael Buehrer, R.M., Arunachalam, S., Wu, K.H, Tonello, A.” Spatial channel model and measurements for IMT-2000 systems”, Vehicular Technology Conference, IEEE VTS 53rd , Volume: 1,Year: 2001, pp342 - 346

[40] Daniel S. Baum, Hansen, J. Salo, J., “An Interim Channel Model for Beyond-3G Systems: Extending the 3GPP Spatial Channel Model (SCM)”, Vehicular Technology Conference, IEEE 61st , Vol. 5, 2005, pp. 3132 – 3136.

[41] Hui Xiao, Burr, A.G., Lingyang Song; "A Time-Variant Wideband Spatial Channel Model Based on the 3GPP Model", IEEE 64th, Vehicular Technology Conference, 2006 pp.1-5.

[42] P. Lusina, Kohandani, F., Ali, S.M.; "Antenna parameter effects on spatial channel models" Communications, IET Volume: 3, Issue: 9, 2009 , pp. 1463 – 1472.

[43] Min Zhang, Peter J. Smith, and Mansoor Shafi. "An Extended One-Ring MIMO Channel, Model", IEEE Transcation on wireless communication, vol. 6, no. 8, aug 2007, pp. 2759- 2764.